Semi-automated measurements of heart-to-mediastinum ratio on ^{123}I-MIBG myocardial Scintigrams by using image fusion method with chest X-ray images

Ryosuke KAWAI[1], Takeshi HARA[1], Tetsuro KATAFUCHI[2], Tadahiko ISHIHARA[3]
Xiangrong ZHOU[1], Chisako MURAMATSU[1], Yoshiteru ABE[4], Hiroshi FUJITA[1]

[1] Department of Intelligent Image Information, Gifu University, Graduate School of Medicine
1-1 Yanagido, Gifu 501-1194, Japan.
[2] Department of Radiological Technology, Faculty of Health Science
Gifu University of Medical Science
795-1 Ichihiraga, Nagamine, Seki, Gifu 501-3892, Japan.
[3] Department of Radiology, Gifu University Hospital, 1-1 Yanagido, Gifu 501-1112, Japan.
[4] Department of Nuclear Medicine-Yaizu City Hospital
1000 Dobara, Yaizu, Shizuoka, 425-0055, Japan.

ABSTRACT

MIBG (iodine-123-meta-iodobenzylguanidine) is a radioactive medicine that is used to help diagnose not only myocardial diseases but also Parkinson's diseases (PD) and dementia with Lewy Bodies (DLB). The difficulty of the segmentation around the myocardium often reduces the consistency of measurement results. One of the most common measurement methods is the ratio of the uptake values of the heart to mediastinum (H/M). This ratio will be a stable independent of the operators when the uptake value in the myocardium region is clearly higher than that in background, however, it will be unreliable indices when the myocardium region is unclear because of the low uptake values. This study aims to develop a new measurement method by using the image fusion of three modalities of MIBG scintigrams, 201-Tl scintigrams, and chest radiograms, to increase the reliability of the H/M measurement results. Our automated method consists of the following steps: (1) construct left ventricular (LV) map from 201-Tl myocardium image database, (2) determine heart region in chest radiograms, (3) determine mediastinum region in chest radiograms, (4) perform image fusion of chest radiograms and MIBG scintigrams, and 5) perform H/M measurements on MIBG scintigrams by using the locations of heart and mediastinum determined on the chest radiograms. We collected 165 cases with 201-Tl scintigrams and chest radiograms to construct the LV map. Another 65 cases with MIBG scintigrams and chest radiograms were also collected for the measurements. Four radiological technologists (RTs) manually measured the H/M in the MIBG images. We compared the four RTs' results with our computer outputs by using Pearson's correlation, the Bland-Altman method, and the equivalency test method. As a result, the correlations of the H/M between four the RTs and the computer were 0.85 to 0.88. We confirmed systematic errors between the four RTs and the computer as well as among the four RTs. The variation range of the H/M among the four RTs was obtained as 0.22 based on the equivalency test method. The computer outputs were existed within this range. We concluded that our image fusion method could measure equivalent values between the system and the RTs.

Keywords: CAD, MIBG, Image fusion, HM ratio, Chest radiograms, Scintigrams, Left ventricle

1. INTRODUCTION

MIBG (iodine-123-meta-iodobenzylguanidine) is a radioactive medicine that is used to help diagnose not only myocardial diseases but also Parkinson's diseases (PD) and dementia with Lewy bodies (DLB) [1, 2]. The quantitative analysis of the uptakes from the myocardium regions in scintigrams is required to discriminate these diseases; however, it is difficult to precisely segment the heart region because the uptake values tend to be very low in PD or DLB patients' images. The difficulty of segmentation often reduces the consistency of the measurement results. One of the most

Medical Imaging 2015: Computer-Aided Diagnosis, edited by Lubomir M. Hadjiiski, Georgia D. Tourassi,
Proc. of SPIE Vol. 9414, 941433 · © 2015 SPIE · CCC code: 1605-7422/15/$18 · doi: 10.1117/12.2081630

common measurements is the ratio of the uptake value of the heart to mediastinum (H/M). This ratio will be stable when the uptake value from the myocardium region is obviously higher than the background signals. However, it may be an unreliable index when the myocardium region is unclear because of the low uptake value to be segmented in the scintigram. This study aims to develop an image fusion technique for MIBG scintigrams and chest radiograms to reduce the inter-/intraoperator variability in measuring H/M in MIBG scintigrams. Furthermore, it aims to construct a statistical atlas for the left ventricular (LV) map by using 201-Tl scintigrams to precisely determine the myocardium region in MIBG scintigrams when the uptake value was low.

2. METHODS

Our automated method consists of the following steps:

(1) Construct LV map from 201-Tl myocardium image database and chest radiograms of anterior-posterior (AP) projections
(2) Determine heart region in chest radiograms
(3) Determine mediastinum region in chest radiograms
(4) Perform image fusion of chest radiograms and MIBG scintigrams by using mutual information of the two images
(5) Perform H/M measurement in MIBG scintigrams by using the heart and mediastinum regions determined from the chest radiograms.

Step (1): Figure 1 shows an overview of constructing the LV map. First, all myocardium regions in the 201-Tl scintigrams were manually extracted by board-certified radiological technologists (RTs). Second, two images of the scintigrams and AP chest radiograms were fused by a manual procedure to determine the myocardium, as shown in Fig. 1(a). All of the myocardium regions were located and were deformed to fit the same typical body shape as shown in Fig.1(b). A no rigid image deformation based on the thin-plate-spline (TPS) method was used for the deformation. Four landmarks (LMs), LM1 to LM4, were automatically detected in the AP chest radiograms. LM1 to LM4 are located between the right-first-arches with right-second-arches, around the last right-second-arches, between the left-third-arches with left-fourth-arches, and the apex of myocardium regions, respectively. After all of the myocardium regions were deformed on the same coordinate in the chest radiogram, the statistical atlas to present the existence probability was constructed as shown in Fig. 1(c) and was used as the LV map.

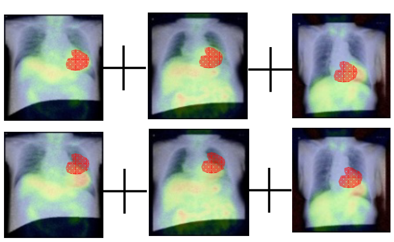

(a) Myocardium region and fused image

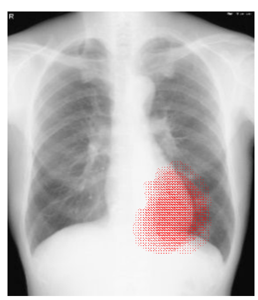

(b) Standardized heart

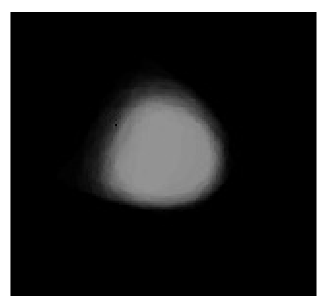

(c) Statistical atlas of left ventricular

Fig. 1 Overview of constructing left ventricular map.

Step (2): To apply the LV map to an objective chest image, the determination of the four LMs was required to deform the shape of the LV map. The LMs were used for the template-matching in the chest X-ray image. The sum of squared difference (SSD) was employed for evaluating the similarity in template-matching. Four template images, as shown in Fig. 2, were used to determine the locations of the four LMs, respectively. LM1, LM2, LM3, and LM4 respectively determine the locations of the upper right, lower right, upper left, and lower left of the heart. The four LMs were searched within limited regions around the heart. The statistical atlas, as shown in Fig.1(c), was deformed to fit the four LMs.

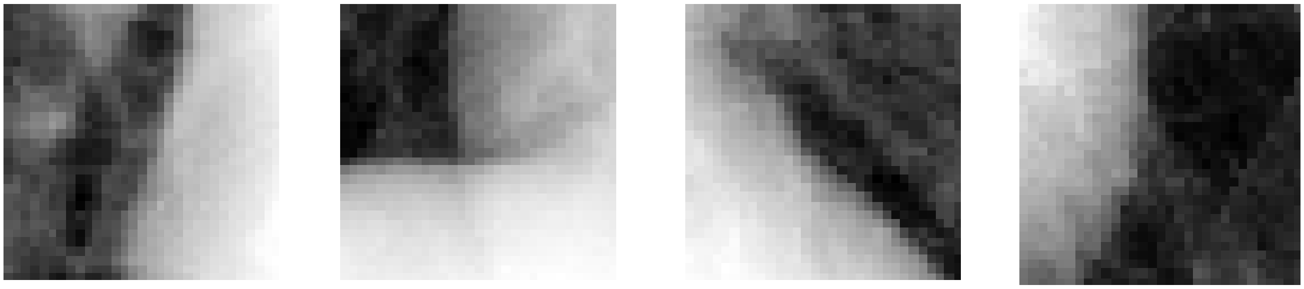

(a) Template for LM1 (b) Template for LM2 (c) Template for LM3 (d) Template for LM4

Fig.2 Template images for landmark determination

Step (3): A median line on the radiograms (green line in Fig. 3(a)) and apexes of the lung (red line in Fig. 3(b)) was determined to locate a mediastinum region. The median line was estimated by using the image profile in the head-tail direction in the chest radiogram. The highest frequency of the profile around the image center was obtained to determine the location of the median line. The apexes were determined by image-thresholding of the chest image. The threshold was determined using the Otsu-method. The top two regions from the largest area except the background were determined as the right and left lung fields. The apexes were considered as the lung apexes. A mediastinum region, shown by the rectangular region in Fig. 3(b) was determined to be slightly below (5 mm) from the intersection point of the apexes of the lung and the median line.

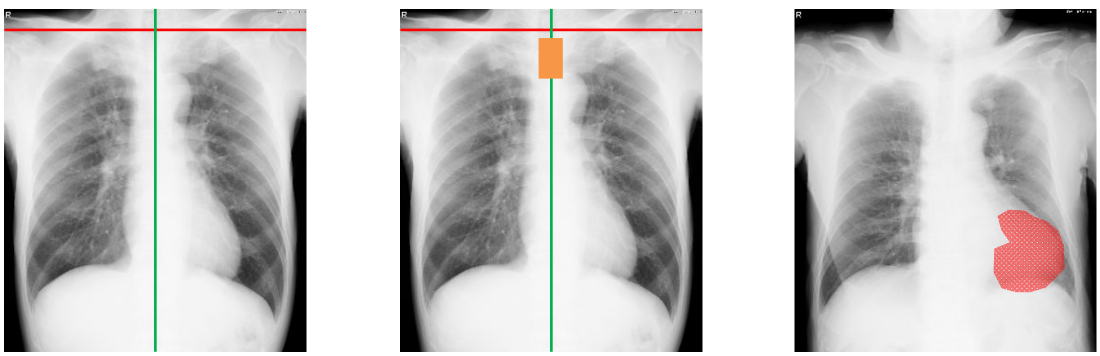

(a) Two determined lines (b) Localized mediastinum region (c) LV region on chest radiogram

Fig. 3 Localization of mediastinum and heart region on chest radiograms

Step (4): To obtain the pixel counts of the mediastinum and heart regions in the MIBG scintigram, the chest radiogram and MIBG scintigram were fused after their image resolutions, inclinations, and the outer area of the body were matched. The image resolution of the two images was matched to 1.16mm x 1.16mm of the scintigram. The mutual information (MI) of the chest radiogram and scintigram was used to determine the alignment for image fusion [3, 4]. After the image fusion of the radiogram and the scintigram, the mediastinum region and LV region were localized in the chest radiogram and the MIBG scintigram.

Step (5): The uptake values in the mediastinum and myocardium regions as the LV region in the scintigrams were obtained based on the fused images. Figure 4(a) shows an example of the fused image of a chest radiogram and an MIBG scintigram. By using this fused result, the mediastinum and myocardium regions were mapped in the scintigram. Figure 4(b) shows two examples with high and low uptakes in the myocardium regions. The mediastinum regions were detected correctly as shown in the examples, and the myocardium regions were also determined correctly irrespective of whether the uptake values of these regions was high or low.

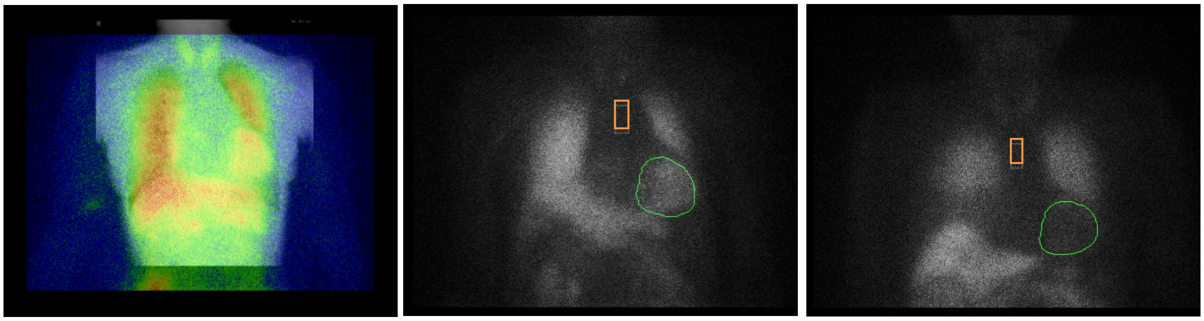

(a) Image of fusion result (b) Mediastinum (orange) and myocardium regions (green)

Fig. 4 Mediastinum (orange) and myocardium regions (green)

3. RESULT

We collected 165 cases with 201-Tl scintigrams and chest radiograms to construct the LV map. Another 65 cases with MIBG scintigrams and chest radiograms were also collected for the measurements. We compared the four RTs' manual results with our computer outputs of H/M for all 65 cases.

48 computer outputs existed in the range of the manual results whereas 17 did not. Of these 17 outputs, 5 and 12 were higher and lower than the manual results, respectively. The maximum and the minimum differences between the four RTs were approximately 0.59 and 0.05, respectively.

Figure 5 shows two examples of the computer outputs with the four RTs' results. The green and red lines indicate the outputs of the computer and the four RTs, respectively. Figure 5(a) shows an example in which the difference between the computer output and the average of the four RTs' results was the smallest, being approximately 0.0. On the other hand, Fig. 5(b) shows an example in which the difference was the largest, being approximately 0.5. The computer output contains the high uptake from the liver region; however, the four RTs skillfully excluded the liver regions when they determined the myocardium region in the scintigram.

Figure 6(a) and (b) also show examples of the two cases from the manual results of the four RTs. Four manual results of the mediastinum and myocardium regions and the H/M measurements by the four RTs are shown in each image. All RTs estimated the myocardium regions in the scintigrams irrespective of whether the uptake was high or not, and well excluded the liver and lung regions.

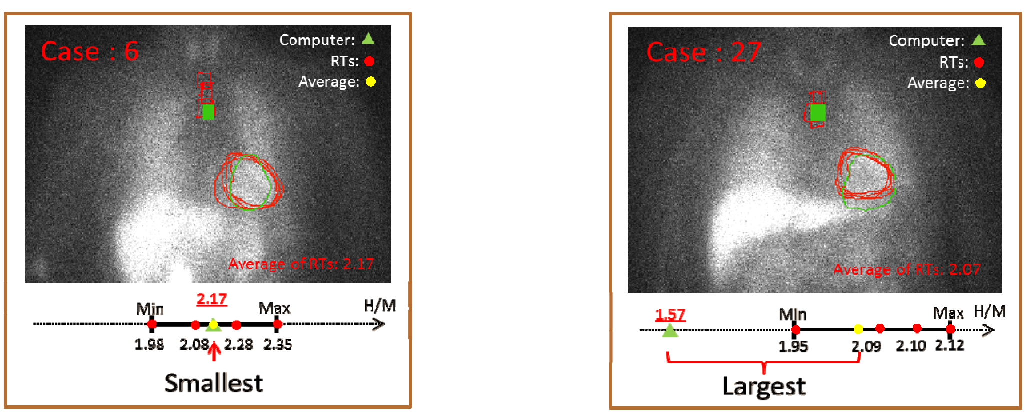

(a) The computer result existed within four RTs' (b) The computer output was quite differ from four RTs'

Fig.5 Comparisons between computer outputs and four RTs' results

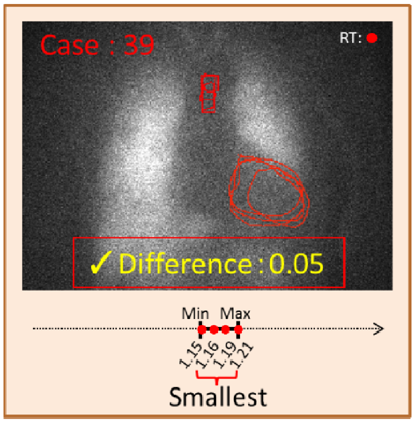

(a) The range of RTs was largest (0.59)

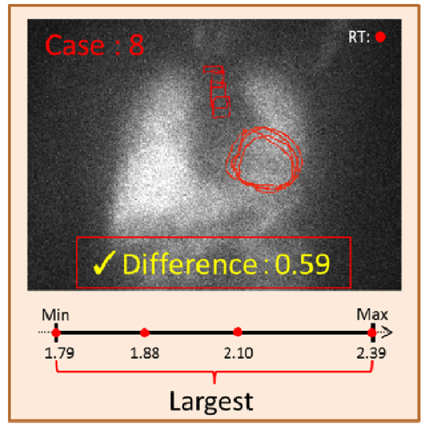

(b) The range of RTs was smallest (0.05)

Fig.6 The ranges between four RTs

4. DISCUSSION

48 of the 65 cases existed within the range of the manual results, but 17 did not. To discuss the difference between the outputs of the computer and the four RTs, we compare the two results by using Pearson's correlation, Bland-Altman method, and equivalence testing.

The correlations of the H/M between the computer outputs and the four RTs' results are shown in Fig. 6(a). The maximum and minimum correlations were 0.88 and 0.85, respectively. The correlations obtained by all six combinations of the four RTs are shown in Fig. 6(b). The maximum and minimum correlations were 0.96 and 0.92, respectively. The largest difference between the computer output the RTs' results and among the RTs was 0.11 (0.85 from Computer vs. RT-C and 0.96 from RT-B vs. RT-D). The computer outputs are considered adequate from the view points of statistical correlations; however, the correlations between the computer and the RTs were actually lower than those among the RTs. Therefore, an analysis of the systematic errors between the computer and the RTs is required to clarify the fixed and proportional biases.

The Bland-Altman method is a well-known approach for showing the systematic errors between two measurement results. The results of the Bland-Altman method between the computer outputs and the RTs' results are shown in Fig. 7(a). The fixed and proportional biases were confirmed in the two combinations. Among the four RTs, the results of the Bland-Altman method showed the same tendency with the existence of fixed and proportional biases in five out of six combinations. This means that systematic errors existed in both of computer vs. RTs and RT vs. RT and the characteristics of the errors were very similar to each other.

Therefore, additional discussions using the equivalency test method are required to by clarify the acceptable ranges of the errors. High correlations and systematic errors existed between the computer outputs and the four RTs' results. The equivalence between the computer and RTs was difficult to prove using Pearson's correlation and the Bland-Altman method. The equivalence test is a common statistical method to clarify the equivalency between two procedures, namely, whether the two results existed within a range to provide the same effects. When the range was configured as the mean difference of the H/M from the four RTs as 0.22, the difference between the computer outputs and the four RTs' results was considered equivalent.

5. CONCLUSIONS

We concluded that the measured values of our computerized method were equivalent to those of the four RTs in terms of the equivalent test with a margin of 0.22.

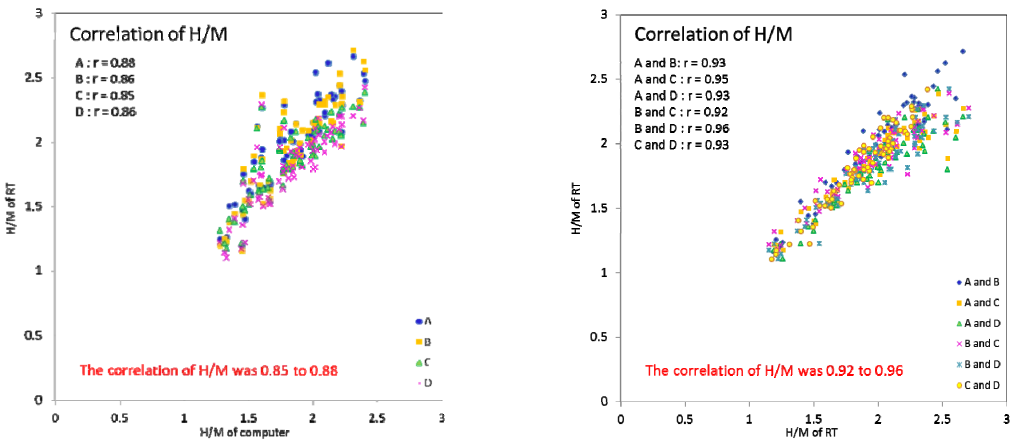

(a) The correlation between computer and four RTs (b) The correlation between RT and RT

Fig.6 Correlation coefficients between computer and RTs

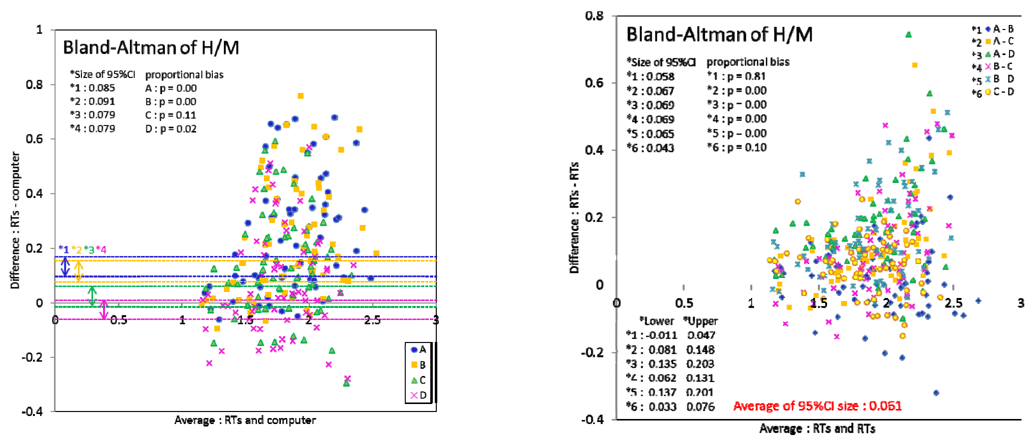

(a) The Bland-Altman between computer and four RTs (b) The Bland-Altman between RT and RT

Fig.7 Systematic errors obtained by the Bland-Altman method

ACKNOWLEDGMENT

This work was partly supported by Grant-in-Aid for Scientific Research(C) 19500385, 23591802, and Grant-in-Aid for Scientific Research on Innovative Areas 21103004 by Japanese Government.

REFERENCES

[1] Satoh, A., Serita, T., Seto, M., Tomita, I., et al., "Loss of 123I-MIBG uptake by the heart in Parkinson's disease: assessment of cardiac sympathetic denervation and diagnostic value", J of Nuclear Medicine, Official Publication, Society of Nuclear Medicine, 40(3), 371-375, (1999).

[2] Yoshita, M., Taki, J., Yamada, M., "A clinical role for [123I]MIBG myocardial scintigraphy in the distinction between dementia of the Alzheimer's-type and dementia with Lewy bodies", J Neurol Neurosurg, 71(5), 583-588, (2001).

[3] Maes, F., Collignon, A., Vandermeulen, D., " Multimodality image registration by maximization of mutual information", IEEE Trans Med Imaging, 16(2), 187-198, (1997).

[4] Watanabe, H., "Image registration and fusion for multimodal medical imaging: Japanese Society of Radiological Technology", 59(1), 60-65, (2003).